IBRO Neuroscience Reports 17 (2024) 252–262

Contents lists available at ScienceDirect

IBRO Neuroscience Reports

journal homepage: www.sciencedirect.com/journal/IBRO-Neuroscience-Reports

Research Paper

Cannabinoid type 2 receptor deficiency leads to Aβ-induced cognitive impairment through promoting microglial sensitivity to Aβ in the prefrontal cortex in mice

Tong Zhang [a], JiaGuang Sun [c], Qiang Jiao [d], ShuaiChen Li [a], XiangBo Meng [a], JingPu Shi [e,*], Bo Wang [b,*]

[a] Department of Stomatology, the First Medical Center, Chinese PLA General Hospital, Beijing 100853, China
[b] State Key Laboratory of Toxicology and Medical Countermeasures, Beijing Institute of Pharmacology and Toxicology, Beijing 100850, China
[c] Department of Anesthesiology, Xingtai People's Hospital, Hebei 054000, China
[d] Henan Institute of Food and Salt Industry Inspection Technology, Henan 450003, China
[e] Department of Anesthesiology, The Fourth Hospital of Hebei Medical University, Shijiazhuang, Hebei 050011, China

ARTICLE INFO

Keywords:
Cannabinoid type 2 receptor
Alzheimer's disease
Neuroinflammation
Microglia

ABSTRACT

Aims: This study is to investigate the effects of Cannabinoid type 2 receptor (CB_2R) deficiency on microglia and cognitive function in both $A\beta_{1-42}$-injected CB_2R knockout mice and a transgenic mouse model of Alzheimer's disease (AD) in brain.

Methods: After hippocampal injection with $A\beta_{1-42}$ oligomers in CB_2R knockout mice with and without CB_2R agonist treatment and in transgenic APP/PS1 mice with CB_2R deletion, the novel object recognition (NOR) and Morris water maze (MWM) tests were performed to assess the animal behavior performance. Immunofluorescence staining was conducted to detect the microglial morphology and activation status. The expression of proinflammation and anti-inflammation cytokines were determined by qRT-PCR.

Results: CB_2R deficiency significantly aggravated cognitive impairment in both $A\beta_{1-42}$-induced and transgenic APP/PS1 animal model in NOR. In Aβ-injected mice lacking CB_2R and transgenic APP/PS1 mice with CB_2R deletion, microglia in the prefrontal cortex exhibited enhanced immunoreactivity with altered morphology. Furthermore, transformation of activated microglial phenotype in the prefrontal cortex was reduced in $A\beta_{1-42}$-injected CB_2R knockout mice after CB_2R agonist treatment. The CB_2R deficiency significantly increased the expression of proinflammatory cytokines in the prefrontal cortex, while it was observed in the hippocampus in both $A\beta_{1-42}$-injected and transgenic APP/PS1 AD mouse model. Furthermore, CB_2R deficiency increased concentrations of soluble $A\beta_{40}$ in the prefrontal cortex, but did not affect plaques deposition.

Conclusion: CB_2R deletion led to enhanced neuroinflammatory responses via direct upregulating microglia activation in the prefrontal cortex during the early symptomatic phase of AD mice. CB_2R modulates prefrontal cortical neuroinflammation, which is essential for regulating cognitive functions such as recognition memory at the early stage of AD.

Introduction

Alzheimer's disease (AD) is the most common form of dementia in the aging population, characterized by the senile plaques, neurofibrillary tangles (accumulated hyperphosphorylated tau), and cerebral amyloid angiopathy. Besides these major neuropathologic hallmarks, the chronic inflammation plays a vital role in the occurrence and development of AD. The astrocytosis and microgliosis represent the two principal neuropathological features of AD. Moreover, microgliosis have been considered as the major component during the prominent inflammatory processes.

Whether microglia have a long term impact on the functional vulnerability of the nervous system? Microglia mediated inflammatory events in brain over the age-related or disease-related progression remain not clear. Thus, much more attention has been paid on the microglial activation and neuroinflammation, inducing the homeostatic

* Correspondence to: Beijing Institute of Pharmacology and Toxicology, 27th Taiping Road, Beijing 100850, China.
E-mail address: 15652507006@163.com (B. Wang).

https://doi.org/10.1016/j.ibneur.2024.08.004
Received 17 April 2024; Received in revised form 8 August 2024; Accepted 17 August 2024
Available online 30 August 2024

imbalance in the CNS during the neurodegenerative pathogenesis (Frank-Cannon et al., 2009; Kwon and Koh, 2020).

In the AD pathogenesis, microglial activation is always induced by soluble β-amyloid peptides (Aβ) oligomers, or insoluble Aβ fibrils (Tomiyama et al., 2010). Active microglia may impact the plaque deposition and maintenance, in a manner temporally and spatially correlating with the microglial number and phagocytic activity in the AD pathogenesis(Bolmont et al., 2008; Meyer-Luehmann et al., 2008). Microglia could exhibit two entirely different functional activating status, referred to as the classical (M1) and alternative (M2) activation, respectively, with the functions switching from deleterious to beneficial. Activated microglia could release pro-inflammatory molecules (such as cytokines, chemokines, and other potential cytotoxic substances), and neurotrophic factors in the brain(Bolmont et al., 2008; Harry and Kraft, 2012). Extensive researches have been performed to understand the molecular mechanisms underlying the microglial function and phenotypical alteration (Meyer-Luehmann et al., 2008). Although the activated microglia showed a uniform distribution throughout the central nervous system (CNS), selective activation of microglia in specific regions of the CNS was found in nerve injury in animal(Zhang et al., 2008). Recent studies indicated microglia played the important role in earlier stages of AD underlying synaptic vulnerability.

Current treatments for AD mainly aim at delaying the disease progresses, including reducing Aβ production, inhibiting Aβ aggregation, and improving Aβ clearance by immunization(Benito et al., 2003; Citron, 2010; Crews and Masliah, 2010; Selkoe, 2001). Emerging evidence suggests that the cannabinoid type 2 receptor (CB_2R)is positively correlated to the pathogenesis of AD, which is more likely to be an important modulator for the neuroinflammation associated with the disease progression(Benito et al., 2003). The Aβ-induced cognitive deficits have been found in the brains of AD patients,CB_2R selective expression in neuritic plaque-associated microglia was demonstrated in regions implicated early in disease progression (hippocampus and entorhinal cortices) in AD patients(Solas et al., 2013). Studies have suggested that the activation of CB_2R is presumed to ameliorate the Aβ burden in AD(Tolon et al., 2009). It has been shown that, the CB_2R deficiency could exacerbate the cortical Aβ deposition and increase the level of soluble $A\beta_{1–40}$(Aso et al., 2013). The CB_2R-mediated effects on microglia are very complex, including stimulating the cell migration and inhibiting the release of various pro-inflammatory cytokines (Miller and Stella, 2008). CB_2R agonists have been shown to be able to ameliorate the cognitive symptoms, through reducing the expression of pro-inflammatory cytokines and GSK3β activity, during the pre-symptomatic stage(Aso et al., 2013) in the APP/PS1 transgenic model mice.But in aged APP/PS1 mice, the CB_2R deficiency leads to reduced microglia and subsequently declined neuroinflammation. Studies have shown the role of CB_2R as an neuroinflammatory mediators in AD(Aso et al., 2016; Morcuende et al., 2022; Stempel et al., 2016). However, the cognitive behavior and Aβ plaques load are independent of CB_2R-mediated neuroinflammation in AD(Schmole et al., 2015). In our previous study using the APP/PS1 transgenic AD mouse model, administration of the CB_2R agonist JWH015for 8 weeks significantly decreased proinflammatory cytokines in the prefrontal cortex but not in the hippocampus(Li et al., 2019)·. Our question is whether microglia are vulnerable to Aβ-induced inflammation in specific brain in early symptomatic stage of APP/PS1 mice? The difference of anti-inflammatory effect of CB_2R agonist related to the vulnerability of microglia still remain unknown. In this study, we adopted bilateral microinjection of $A\beta_{1–42}$ fibrils into the hippocampal CA1 area of CB_2R knockout mice to identify the critical role of microglial CB_2R in different brain region. Furthermore, the constitutive role of microglial CB_2R in early symptomatic stage of APP/PS1 transgenic AD mouse model was investigated.

Methods

Experimental animals

Transgenic APP/PS1 (APPswe and PS1dE9) mice and CB_2R knockout ($CB_2R^{-/-}$) mice were originally purchased from the Jackson Laboratories (Bar Harbor, Maine, USA). $CB_2R^{-/-}$ mice were crossed with the C57BL/6 J mice to generate the heterozygous $CB_2R^{+/-}$ mice. The obtained $CB_2R^{+/-}$ mice were bred with each other to get the littermates of $CB_2R^{-/-}$mice and the related control animals. APP/PS1 mice were then crossed with $CB_2R^{-/-}$ mice. APP/PS1*$CB2^{+/-}$ mice were then crossed with $CB_2R^{-/-}$ mice. The experiments were carried out on the mice at age of 6 month, i.e., at the early-symptomatic stage(Aso et al., 2013). All animals were subjected to the novel object recognition (NOR) test and the Morris Water Maze (MWM) test.

These mice were subjected to the genotyping with PCR using primers as described in Supplementary Table 1. Animal experiments were conducted in accordance with the National Institute of Health Guide for the Care and Use of Laboratory Animals (NIH Publications No. 80–23), and were approved by the Animal Care and Use Committees of Beijing Institute of Pharmacology and Toxicology (IACUC-DWZX-2021–723).

Experimental materials

The selective CB_2R agonist, JWH-015 (the Ki values for CB_1R and CB_2R were 383 nM and 13.8 nM, respectively), was purchased from Sigma-Aldrich (St. Louis, MO, USA), initially dissolved in dimethyl sulfoxide (DMSO), at the concentration of 16.67 mg/mLas stock. Before administration, JWH-015 was further diluted with saline, containing 1 % DMSO and 1 % Tween 80.

Experimental design

Based on genotypes and treatments, the animals received vehicle or JWH-015 at a dose of 0.5 mg/kg, i.p., daily for 7 days, which were then injected with $A\beta_{1–42}$ fibrils or saline into the CA1 region of hippocampus followed by pharmacological treatment for another 7 days (See experimental timeline Fig. 1A).The animals were divided into the following 6 groups: $CB_2R^{-/-}$ mice injected with $A\beta_{1–42}$ fibrils and 0.5 mg/kg JWH-015 i.p. daily for 14 days (KO+Aβ+JWH) or vehicle i.p. daily for 14 days (KO+Aβ+VEH), respectively. C57BL/6 J mice injected with $A\beta_{1–42}$ fibrils and 0.5 mg/kg JWH-015 i.p. daily for 14 days (Ctrl +Aβ+JWH) or vehicle i.p. daily for 14 days (Ctrl +Aβ+VEH), respectively. C57BL/6 J control group and $CB_2R^{-/-}$ mice control group received bilateral microinjection of saline and vehicle i.p. daily for 14 days, (Ctrl +NS+VEH) and (KO+NS+VEH), respectively. All animals were subjected to the novel object recognition (NOR) test and the brains were removed and frozen at −80℃for further analysis.

Aβ preparation and Aβ-injected AD model establishment

The $A\beta_{1–42}$ peptide was purchased from the Bachem Company (Haupstrasse, Switzerland), and dissolution was prepared according to the manufacture's instructions. Briefly, 500 μL $A\beta_{1–42}$ powder was incubated in 200 μL saline at 37℃ for 7 days and stored at −80℃. Before injection, $A\beta_{1–42}$ oligomers were diluted with saline, to obtain the final concentration of 11 μg/μL.

Both the CB_2R knockout mice and their control mice (aged 10 weeks) were anesthetized deeply with sodium pentobarbital (45 mg/kg, i.p.), which were restrained in a stereotaxic apparatus. Totally 2 μL synthetic human $A\beta_{1–42}$ peptide (1 μg/μL) or NS was injected stereotaxically and bilaterally into the CA1 region of hippocampus, according to the following coordinates: bregma, −2.0 mm anteroposterior, ±2.0 mm mediolateral, and −2.3 mm dorsoventral. The injection was undertaken using a 10-μl Hamilton syringe, and driven by the microsyringe pump controller, at a rate of 0.2 μl/min, followed by the pause for another

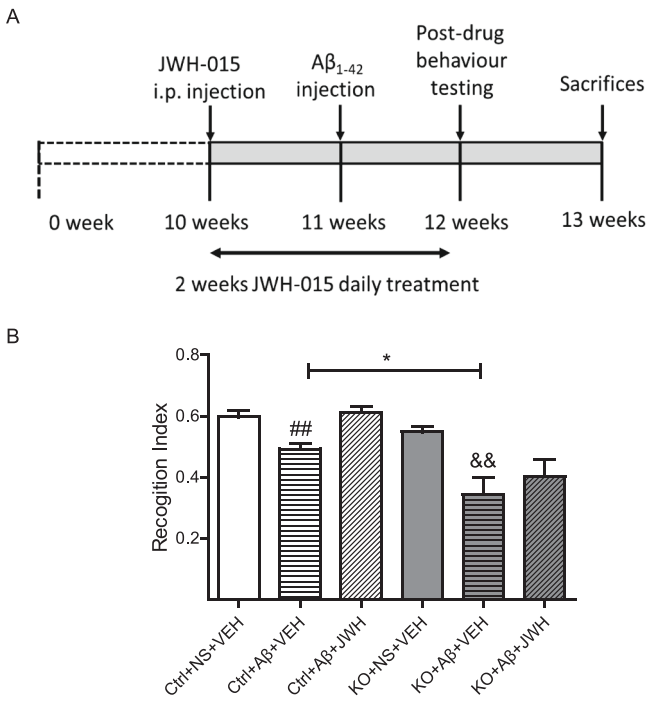

Fig. 1. The cognitive performance of CB2R KO mice injected with $A\beta_{1-42}$ was measured by the two-object recognition test. (A) Timeline of experimental animal design of intrahippocampal Aβ-injected AD mouse model. (B) The recognition index (RI) of vehicle-treated or JWH-015 treated control mice and CB_2R-/-(KO) mice with or without intrahippocampal injection of Aβ. The Ctrl+Aβ+VEH group showed a significant decrease compared with Ctrl+NS+VEH group ($^{\#\#}P<0.01$) , as well as the KO+Aβ+VEH group compared with KO+NS+VEH group($^{\&,\&}P<0.01$). Data were analyzed by Student t-test. Data are expressed as mean±SEM (n=15–20). The RI value of KO+Aβ+VEH group was significantly decreased ($^{*}P<0.01$) compared with Ctrl+Aβ+VEH group. JWH-015 treatment was not able to modify the recognition impairment of CB_2R KO mice with intrahippocampal injection of Aβ. Data were analyzed by Two-way ANOVA.

5 min to prevent the leakage. The animals were allowed to recover on a heating pad completely, which were returned to the animal facility.

Novel object recognition (NOR) test

This paradigm was performed under dim light, in an open plastic arena (45 cm × 35 cm × 20 cm), which was monitored by a video-camera. The test was conducted over 3 days by an investigator blinded to the animal grouping and drug administration. On the first day, mice were habituated to the empty arena for 20 min. On the second day, mice were returned to the same arena containing two identical objects, and allowed for exploration for 6 min. On the third day, one of two familiar objects was replaced by a novel one, with the different shape, color, and material. Mice were allowed to explore the arena for 6 min, and total time exploring each object was recorded. Exploration was defined as nosing and sniffing the object, at a distance less than 2 cm, excluding lying on it or passing by unintentionally. Objects and arena were cleaned thoroughly after each trial. The recognition index (RI) was calculated as the time exploring the novel object divided by the total time exploring the two objects. Mice with the non-spatial memory impairment would show a lower RI value.

Morris water maze (MWM) test

Spatial learning and memory of mice was assessed by the MWM test. The maze consisted of an open-field circular pool, which was filled with water at approximately 24℃ to the depth of 30 cm. The pool was divided into four equal quadrants. A white escape platform (10 cm in diameter) was submerged in the center of one quadrant, 1.5 cm beneath the water surface. The maze was completely separated from the surroundings with a black curtain to decrease the interfering. A video-camera located above the maze was used to record the tracking of mice, and the data were analyzed with the Dig-Behav software (Jiliang Co., Ltd., Shanghai, China).

The place navigation test was performed for each animal, with 4 trials per day for 5 consecutive days. The time landing the platform was recorded and calculated as the escape latency. In each trial, mice were released into the water, in the position of facing the wall, from 4 fixed different sites randomly. They were allowed to swim freely until climbing onto and staying on the platform for 10 sec, within 60 sec. If they failed to find the platform, the mice would be guided to the platform for 10 sec. The swimming speed was also recorded. During the spatial probe test (on the sixth day), the escape platform was removed. All animals were placed into the pool as previously, and allowed to swim freely for totally 60 sec. The times of crossing the former platform were recorded and analyzed.

Immunofluorescence staining

A cohort of mice (4–5 per group) were deeply anesthetized and transcardically perfused with 4℃ PBS, followed by perfusion with 4 % paraformaldehyde (PFA) in PBS. The brain tissues were rapidly removed and fixed in 4 % PFA overnight, and then transferred into 30 % sucrose in PBS for 3 days. The tissues were continuously cut into 20-μm coronal frozen section series on a Leica cryostat (Leitz, Germany).

After antigen retrieval of microwave in citrate for 15 min, the coronal sections were subsequently incubated with 3 % BSA and 0.3 % Triton X-100 PBS at room temperature. For the double-labeling immunofluorescence staining, the sections were incubated with primary antibodies at 4℃ overnight. Primary antibody pairs and working conditions were as follows: mouse monoclonal anti-Aβ (1:50 dilution; Convance, Princeton, NJ, USA) with rabbit polyclonal anti-Iba1 (1:500; Abcam, Cambridge, MA, USA); rabbit polyclonal anti-Aβ (1:50 Abcam, USA) with mouse monoclonal anti-GFAP (1:500, Millipore, USA). After complete rinsing with PBS, sections were incubated with appropriate Alexa 488- or 594-conjugated fluorescence secondary antibodies against corresponding host species. Thereafter, the nuclei was stained with 4'-6'-diamidino-2-phenylindole dihydrochloride (DAPI; Boster, Wuhan, Hubei, China). Negative control was performed in alternate sections with no treatment of primary or secondary antibodies.

Fluorescence examination of Iba1-labeled microglia and GFAP labeled astrocyte was performed using the Nikon Eclipse Ni microscope equipped with a digital color camera (Jenoptik I Optical Systerm, Germany). Representative pictures of hippocampus and overlying prefrontal cortex were taken at 10× or 20× magnification in a blind manner, and the integrated optical density per slice (5–6 sections per group) was measured using the image pro primer 3D software. The morphology of microglia cells around the Aβ injection site in the prefrontal cortex were detected and assessed under the Zeiss LSM 510 meta confocal microscope at the 100× magnification. This experiment was carried out in triplicates.

Quantitative real-time PCR

After deeply anesthetized, the brain tissues were rapidly removed from the mice after perfusion with 4℃ PBS. Prefrontal cortex and hippocampus were dissected on an ice-cold glass dish, and immediately placed into the RNA fixer solution (Biomed, Beijing, China). Total RNA was extracted using the RNeasy Mini kit (Qiagen, Valencia, CA, USA), according to the manufacturer's instructions. Reverse transcription for cDNA was undertaken with the ReverTra Ace qPCR RT Master Mix with gDNA Remover kit (Toyobo, Osaka, Japan), according to the manufacturer's instructions. Quantitative real-time PCR was performed using the

Fast Start Essential DNA Green Master kit (Roche Diagnostics, Mannheim, Germany) on Roche Light Cycler. The primers were synthesized by the Invitrogen company as listed in Supplementary Table 2, including the M1 microglia markers (IL-6, TNF-α, and iNOS), M2 microglia marker (Ym1/2), and housekeeping gene (GAPDH). Totally 50 ng cDNA was used per reaction, and the amplification conditions were as follows: 95℃ for 10 min; 95℃ for 10 sec, and 60℃ for 1 min, for 45 cycles. The mRNA expression levels of interest genes were calculated with the $2^{-\triangle\triangle ct}$ method, and normalized against GAPDH as internal reference.

Enzyme-linked immunosorbent assay

Tissues of hippocampus and cortex were dissected, weighed and sonicated in ice-cold DEA buffer (10 μL/mg tissue; 0.2 % diethanolamine in 50 mM NaCl). The lysate was centrifuged at 12,000 × g for 20 min at 4 °C). The supernatant was collected for measuring mouse $A\beta_{40}$ and mouse $A\beta_{42}$ (pg/ml mg protein) according to the manufacturer's instruction by using ELISA kits (mouse Aβ40 ELISA Kit, KMB3481; mouse Aβ42 ELISA Kit, KMB3441; Thermo Fisher Scientific). All ELISAs were read on a microplate reader (Synergy H1; BioTek; Agilent) at 450 nm.

Congo red staining

Congo red staining was conducted according to the manufacture's protocol (Sigma Aldrich, St. Louis, MI). Briefly, 20 μm thick coronal sections were rehydrated and incubated in alkaline sodium chloride solution for 20 min at room temperature. NaOH solution was added to freshly prepared and filtered Congo red solution, then sections were stained in this solution for 20 min at room temperature followed by Mayer's hematoxlyin counterstaining (Sigma-Aldrich, St. Louis, MI). Digital images of the hippocampus and overlying cortex of Congo red stained sections were taken using an Olympus VS120 microscope at 4× magnification.

Statistical analysis

Data were expressed as mean ± SEM. Statistical analysis was conducted using the Prism 5 software (GraphPad Software Inc., San Diego, CA, USA). Comparison was performed with student *t*-test or the Two-way ANOVA followed by Tukey's post hoc when required. $P < 0.05$ was considered statistically significant.

Results

Exacerbated cognitive impairment in $A\beta_{1-42}$-injected CB_2R knockout mice

To understand whether the cognitive impairment of $A\beta_{1-42}$-injected mice was affected by the CB_2R deletion, the animal cognitive behavior was first examined using the novel-object recognition test. The effects of CB_2R agonist JWH-015 on Aβ-induced memory performance in mice with and without CB_2R were also investigated. As shown in Fig. 1, our results indicated significantly reduced recognition index (RI) values for Ctrl +Aβ+VEH mice ($p<0.01$) compared to that of Ctrl +NS+VEH mice. Similarly, KO +Aβ+VEH mice had a significantly lower RI compared to that of KO+Aβ+VEH mice ($p<0.01$). The results from the two-way ANOVA revealed KO +Aβ+VEH mice had a significantly lower RI compared to that of Ctrl +Aβ+VEH mice ($p<0.05$). The memory impairment was observed in KO +Aβ+VEH mice on the NOR test when compared to Ctrl +Aβ+VEH mice. The JWH-015 treatment showed slightly modify the recognition impairment of Ctrl +Aβ+VEH mice although the observed difference was not statistically significant.

Increased microglial immunoreactive response to $A\beta_{1-42}$ injection in CB_2R knockout mice

To elucidate the mechanism underlying the increased cognitive impairment of the $CB_2R^{-/-}$ mice induced by $A\beta_{1-42}$, the activated microglia and astrocytes were assessed with Iba1 and GFAP staining.

Notably, the Iba-1 immunostaining demonstrated rather unique alterations in the morphological phenotypes of microglia, transforming from ramified morphology with slender projecting processes to multipolar morphology with more ramifications, in the Ctrl +Aβ+VEH mice. Ramified microglial cells with larger soma, as well as thick and radially projecting processes with more fine ramifications, were also observed in KO +Aβ+VEH mice (Fig. 2A).

As shown in Fig. 2B, the Iba1 intensity was significantly increased in the prefrontal cortex of both Aβ-injected control and $CB_2R^{-/-}$ mice, compared with mice of corresponding genotype injected with saline ($p<0.01$) respectively] (Fig. 2B). Moreover, two-way ANOVA revealed significant effects for the genotype [$F(1, 18) = 4.995$, $P<0.05$]. KO +Aβ+VEH mice showed more enhanced microglial immunoreactivity intensity in the prefrontal cortex, compared with Ctrl +Aβ+VEH mice ($p<0.05$). Furthermore, when compared to Ctrl +Aβ+VEH mice, the JWH-015 treatment significantly reduced the enhancement of Iba1 intensity in Ctrl +Aβ+JWH mice ($p<0.01$). However, no significant differences were observed in the astrocyte immunoreactivity between these groups (Suppl. Fig. 1).

Increased inflammatory responses to $A\beta_{1-42}$ injection in CB_2R knockout mice

To assess the impact of CB_2R deficiency on the microglial function, the cytokine markers for microglial activation were further analyzed in the the prefrontal cortex in$CB_2R^{-/-}$ mice induced by $A\beta_{1-42}$, including the pro-inflammatory markers (IL-6, TNF-α, and iNOS) and anti-inflammatory marker (Ym1/2). As shown in Fig. 3, compared with Ctrl +NS+VEH mice, the mRNA levels of IL-6 were significantly increased in Ctrl +Aβ+VEH mice ($P<0.001$). Similarly, compared with KO +NS+VEH mice, most dramatic increases were observed in the mRNA levels of IL-6of the $CB_2R^{-/-}$ mice ($P<0.001$), Similarly, our results showed that the mRNA levels of TNF-α were significantly increased in both Ctrl +Aβ+VEH mice and KO+Aβ+VEH mice, compared with corresponding Ctrl +NS+VEH mice ($P<0.001$) and KO+Aβ+VEH mice ($P<0.001$), respectively. However, no significant effects of genotype was observed in the mRNA expression levels of iNOS, although there was a slight increase in both Ctrl +Aβ+VEH mice and KO+Aβ+VEH mice, compared with corresponding Ctrl +NS+VEH mice ($P < 0.001$) and KO +NS+VEH mice ($p = 0.0507$), respectively Meanwhile, the Ym1/2 mRNA expression levels exhibited significant reduction in both Ctrl +Aβ+VEH mice and KO+Aβ+VEH mice, compared with corresponding Ctrl +NS+VEH mice and KO +NS+VEH mice (both $p<0.05$). Moreover, compared with Ctrl + Aβ+VEH mice, the increased mRNA expression levels of IL-6 and TNF-α were significantly reduced by the JWH-015 treatment in the Ctrl +Aβ+JWH mice (both $p<0.01$),the reduced the Ym1/2 mRNA levels was partially reversed by the JWH-015 treatment in the Ctrl +Aβ+JWH mice, although the difference was not statistically significant. Two-way ANOVA revealed significant effects for the genotype [$F(1, 16)=7.51$, $p<0.05$] concerning the IL-6 level and the TNF-α mRNA expression level [$F(1, 16)=10.5$, $p<0.01$], KO +Aβ+VEH mice showed significantly increase in both the IL-6 and the TNF-α mRNA expression level compared with KO +Aβ+VEH mice ($p<0.05$ and $p<0.01$, respectively), thus CB_2R deletion increased the microglial immunoreactivity in the prefrontal cortex.

CB_2R deficiency leads to cognitive impairment in APP/PS1 mice

The APP/PS1 mice were bred with the $CB_2R^{-/-}$ mice, both the NOR test and the Morris Water Maze test were assessed during the early

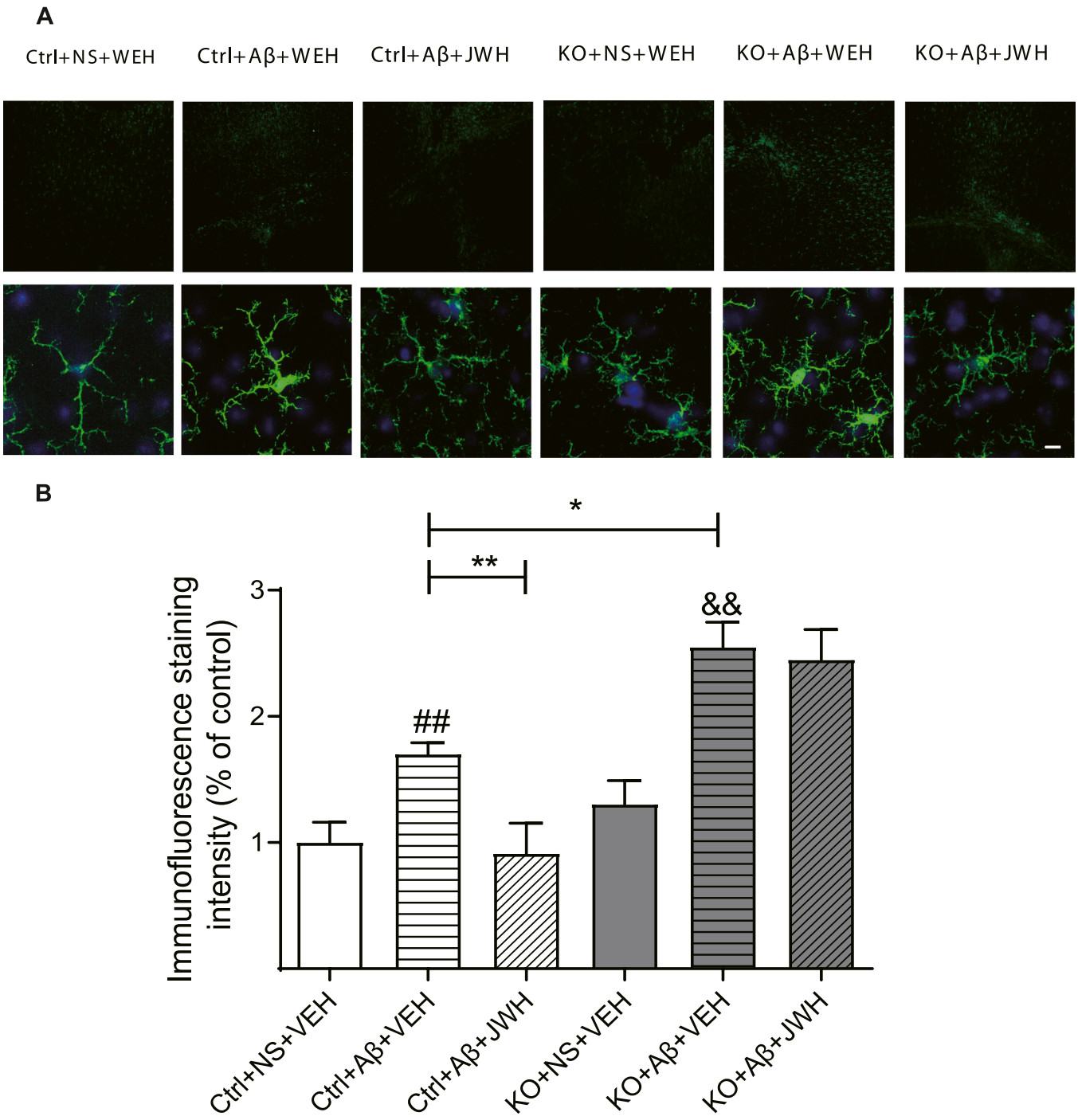

Fig. 2. Microglial cell activation accompanied by morphological difference was measured by Iba-1 immunofluorescence staining in the prefrontal cortex in CB2R KO mice. (A) Representative immunofluorescence images of microglia in the prefrontal cortex of vehicle-treated or JWH-015 treated control mice and CB_2R-/-mice with or without intrahippocampal injection of Aβ. Activated microglia were visualized with ionized calcium-binding receptor adapter molecular 1 antibody (Iba-1) in green and nuclei were stained with 4'-6-diamidino-2-phenylindole dihydrochloride (DAPI) in blue. Scale bar represents 100μm(original magnification 10×) in first line. Panels to the right show high-magnification images of the cortical areas in the left panels. Scale bar represents 10μm (original magnification 100×) in second line. (B) Quantification of Iba-1 immunofluorescence intensity of all groups, presented as percentage of Ctrl+NS+VEH group. $^{\#\#}P<0.01$ compared with Ctrl+NS+VEH group, $^{\&,\&}P<0.01$ compared with KO+NS+VEH group. Data were analyzed by Student t-test. $^{*}P<0.01$, $^{**}P<0.01$ compared with Ctrl+Aβ+VEH group. Data were analyzed by Two-way ANOVA. Results are expressed as mean±SEM (n=15–20).

symptomatic phase of AD mice. Similar observation was seen in the NOR test, APP/PS1*$CB_2R^{-/-}$ mice had a significantly lower RI value compared to that of APP/PS1 mice ($p < 0.05$), indicative of the dramatic memory impairment (Fig. 4A). Moreover, the two-way ANOVA revealed significant effects for the CB_2R deletion [$F(1,32)=7.15$, $p<0.05$] and the APP/PS1 transgene [$F(1,32)=9.66$, $p<0.001$)], but without interaction between the two genotypes. In the MWM test, the APP/PS1*CB_2R-/-mice showed a significantly longer latency to reach the platform compared with the APP/PS1 mice (Fig. 4B, $p < 0.05$) on day 5. The two-way ANOVA revealed a significant effect for the CB_2R deletion on the acquisition of the task [$F(1,31)=4.198$, $p<0.05$]. In the probe trial on day 6, APP/PS1*$CB_2R^{-/-}$ mice showed less time spent less platform-

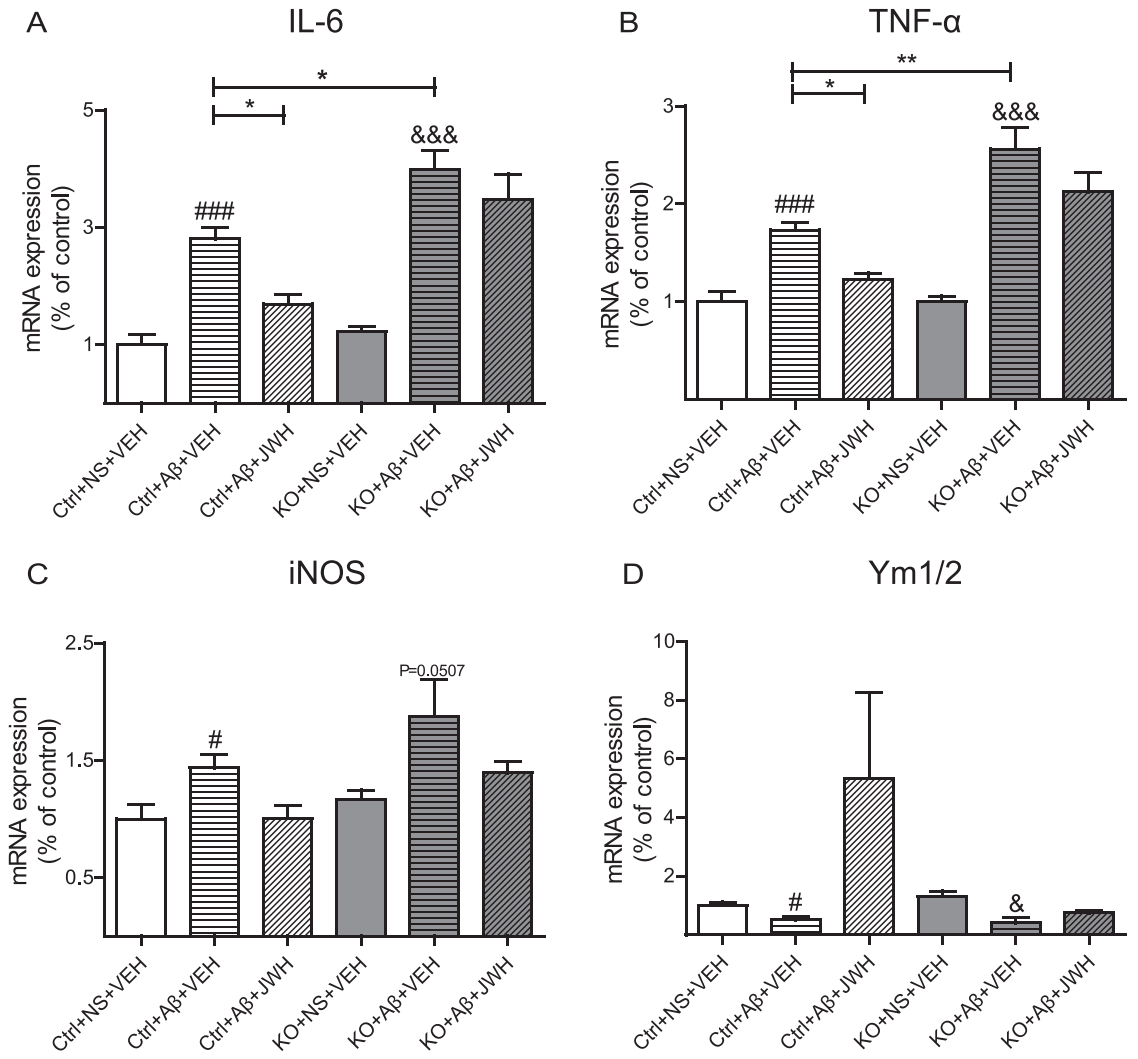

Fig. 3. Proinflammatory mediators mRNA expression level in the prefrontal cortex in CB2R KO mice injected with $A\beta_{1-42}$ assessed by quantitative real-time PCR. Quantification of IL-6(A), TNF-α(B), iNOS(C) and Ym1/2(D) mRNA levels in the prefrontal cortex of vehicle-treated or JWH-015 treated control mice and CB_2R-/- mice with or without intrahippocampal injection of Aβ.The mRNA expression levels of interest genes were normalized against GAPDH and presented as percentage of Ctrl+NS+VEH group. $^{\#}P<0.05$, $^{\#\#\#}P<0.001$ compared with Ctrl+NS+VEH group, $^{\&}P<0.05$, $^{\&,\&,\&}P<0.001$ compared with KO+NS+VEH group. Data were analyzed by Student t-test. $^{*}P<0.01$, $^{**}P<0.01$ compared with Ctrl+ Aβ+VEH group. Data were analyzed by Two-way ANOVA.Results are expressed as mean±SEM (n=8–10).

passing times and less platform-passing times in the target quadrant, although the observed difference was not statistically significant (Fig. 4C, D). We noted that CB_2R deletion had a detrimental effect on spatial learning and memory in 6-month-old APP/PS1 mice.

CB_2R deficiency leads to increased microglial inflammation and differential microglial activation status in APP/PS1 mice

To investigate whether the microglial activation and morphological phenotypes were affected by the CB_2R deletion, the microgliosis in the prefrontal cortex and hippocampus was assessed using the immunohistochemical staining for Iba-1. As shown in Fig. 5A-B, significantly increased Iba-1 immunoreactivity was observed in the prefrontal cortex surrounding the amyloid plaques in the APP/PS1*$CB_2R^{-/-}$mice, compared with the APP/PS1 mice ($P<0.05$). The two-way ANOVA revealed significant effects for the CB_2R deletion [$F(1,15)=13.56$, $p<0.05$]). However, there was no significant difference in the Iba-1 immunoreactivity in the hippocampus between these two groups (Fig. 5C). On the other hand, the morphological phenotypes of the microglial cells in the prefrontal cortex were observed with confocal laser scanning microscopy. As shown in Fig. 5D, ramified microglial cells with long and thin radially projecting processes were mainly observed in the APP/PS1 and APP/PS1*$CB_2R^{-/-}$ mice. Interestingly, in the APP/PS1 mice, majority of ramified microglial cells were mono-polarized, with ramifications extending toward one direction. As expected, in the APP/PS1*$CB_2R^{-/-}$ mice mice, more ramified microglial cells with thick projecting processes were observed. However, no significant difference was observed concerning the GFAP immunoreactivity in either the prefrontal cortex or hippocampus between these two groups (Suppl. Fig. 2).

CB_2R deficiency leads to increased inflammatory responses in APP/PS1 mice

Based on the findings that CB_2R deletion in the APP/PS1 mice impacted the microgliosis in prefrontal cortex, the mRNA expression levels of pro-inflammatory cytokine IL-6, TNF-α, and iNOS were next investigated in the APP/PS1 and APP/PS1*$CB_2R^{-/-}$ mice mice (aged 6 months). As shown in Fig. 6A, the two-way ANOVA reveled significant effects for genotype [for APP, $F(1,14)=35.04$ and $p<0.001$; and for CB_2R deletion, $F(1,14)=5.7$ and $p<0.05$), as indicated the increased IL-6 mRNA level in the APP/PS1 mice compared with the wild-type control mice ($P<0.01$). As expected, compared with the APP/PS1 mice,

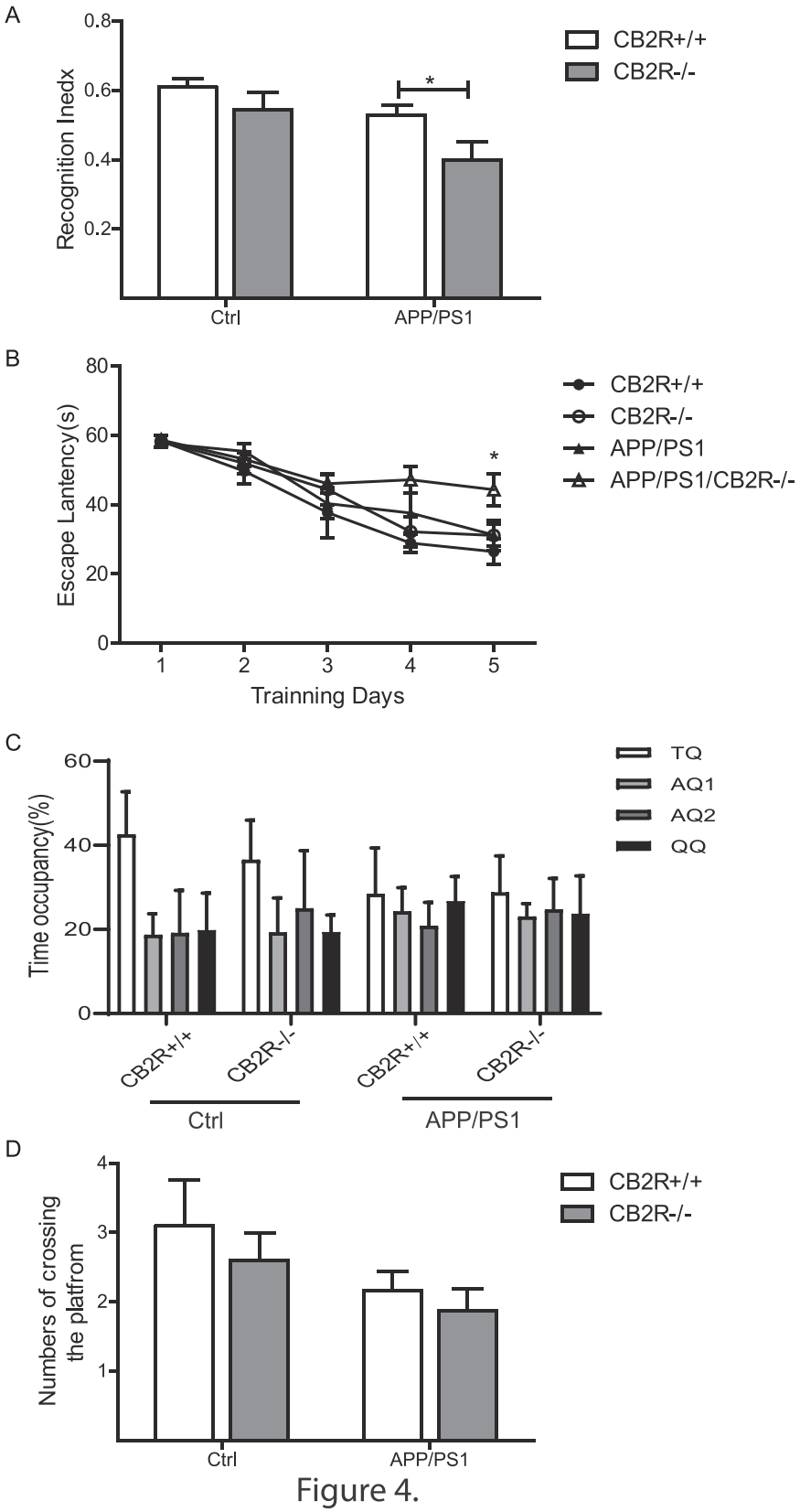

Figure 4.

(caption on next page)

Fig. 4. CB_2R deletion led to accelerated cognitive impairment in APP/PS1 mice. The cognitive performance of APP/PS1 mice with CB2R deletion was measured using two-object recognition test (A) and Morris water maze test (B、C、D). (A) APP/PS1*$CB2R^{-/-}$ mice showed a significantly lower RI when compared to APP/PS1 mice. (B) The escape lantency time of APP/PS1 mice (white triangles), APP/PS1/$CB2R^{-/-}$ mice (black triangles), Control mice (white circles), and $CB2R^{-/-}$ mice (black circles) at 6 months of age was shown on 5 consecutive days. Significant difference was found between APP/PS1 mice with APP/PS1*$CB2R^{-/-}$ mice on day 5 (*$P<0.05$). (C)The probe trial was performed on day 6 to determine the time spent in the target quadrant (TQ or platform quadrant) compared with right quadrant (RQ), opposite quadrant (OQ), and left quadrant (LQ) , and (D) the numbers of crossing the platform were counted in each group. Data were analyzed by Two-way ANOVA. Results are expressed as mean±SEM (n=10–12).

significantly increased IL-6 mRNA level was observed in the APP/PS1*$CB_2R^{-/-}$ mice ($p<0.05$). Furthermore, the TNF-α mRNA levels also exhibited a dramatic increase in the prefrontal cortex in the APP/PS1*$CB_2R^{-/-}$ mice($p<0.01$), compared with the APP/PS1mice mice, even though no significant difference was observed between 6-month-old wild-type control mice and APP/PS1 mice. The two-way ANOVA reveled significant effects for the CB_2R deletion effect [$F(1,12)=10.57$, $P<0.01$] and the APP transgene [$F(1,12)=14.65$, $p<0.01$] (Fig. 6B). However, in the hippocampus, an increase of IL-6 mRNA level was observed in the APP/PS1*$CB_2R^{-/-}$ mice ($p<0.01$), compared with the APP/PS1 mice, as revealed with the two-way ANOVA analysis [for the CB_2R deletion, $F(1,12)=6.58$, $p<0.05$) (Fig. 6D). In addition, the TNF-α mRNA level exhibited an increasing tendency, even though with no statistical significance (Fig. 6E). However, no significant differences were observed in the iNOS mRNA expression level, either in the prefrontal cortex, or in the hippocampus (Fig. 6C and F).

Discussion

In this study, our results suggested that the CB_2R deletion led to significantly impaired performance in the prefrontal cortex (PFC)-dependent object recognition task and lower extent memory deficits in the hippocampus-dependent spatial taskin AD models. In the non-spatial object-recognition task, the Aβ-injected $CB_2R^{-/-}$ mice displayed significantly attenuated exploration for the novel objects compared with the Aβ-injected control mice. The attenuated cognitive performance of the Aβ-injected $CB_2R^{-/-}$ mice could not be reversed when treated with JWH-015. Furthermore, the 6-month-old CB_2R-deficient APP/PS1 mice also showed more severe cognitive impairment, compared with the APP/PS1 mice. In our study, the abilities of $CB_2R^{-/-}$ mice in the spatial navigation of the MWM task remain controversial. Compared with the Aβ-injected control mice, the Aβ-injected $CB_2R^{-/-}$ mice did not display severe cognitive deficits, with longer escape latency in the MWM test and more target crossings in the probe trial (data not shown). Because of this Aβ-induced AD model, we were not convinced that the observed deficits in the $CB_2R^{-/-}$ mice were due to the inability to utilize the spatial information to locate the platform. Nevertheless, compared with the APP/PS1 mice, CB_2R-deficient APP/PS1 mice displayed the longest escape latency to find the platform during the training trails, only on day 5. Moreover, the CB_2R-deficient APP/PS1 and APP/PS1 mice did not recall the location of the former platform during the probe trail. The robust effects suggested that the non-spatial memory was more sensitive to CB_2R deletion during the early symptomatic stage of AD than the spatial memory. The object recognition task is, to a great extent, dependent on the prefrontal cortex and perirhinal cortex Irit and Mouna, 2006). However, the spatial memory in the MWM task heavily relies on the dorsal CA1 area in the hippocampus(Morris et al., 2006; Rossato et al., 2006). The differential effects might probably be due to the greater sensitivity of the prefrontal cortex than the hippocampus to the Aβ-induced cognitive deficits when CB_2R was deleted. Hence, our results showed that the effects of CB_2R deletion on Aβ-induced cognitive impairment depended on the specific task and affected brain region in mice.

Meantime, our results demonstrated that the chronic treatment of JWH-015 had positive effects on the declined cognitive function in Aβ-induced animal models. In line with these findings, previous reports(Aso et al., 2013; Martin-Moreno et al., 2012) have shown that the chronic treatment of JWH-133 induces the cognitive improvement in the 3-month-old APP/PS1 mice in the object recognition task. These results suggested that the stimulation of CB_2R ameliorated the impaired memory and learning functions at the pre-symptomatic stage of AD.

Whether the severe decline in cognitive behavior in the CB_2R-deficient APP/PS1 mice was closely related to microglia-mediated dysfunctional inflammation were also clarified. Our results showed that more robustly microglial activation was observed in the prefrontal cortex in the Aβ-induced $CB_2R^{-/-}$ mice and CB_2R-deficient APP/PS1 mice, than the Aβ-injected WT mice and APP/PS1 mice, respectively. Unexpected, hippocampal Iba-1 immunoreactivity was unaffected by the CB_2R deletion in the APP/PS1 mice. Microglia can be activated by Aβ (Nakajima and Kohsaka, 2001). Active microglia may contribute to the neuronal damages by generating free oxygen radicals and nitric oxide (NO), and releasing the potentially neurotoxic cytokines (such as TNF-α). Cytokines involved in the inflammatory cascades are also supposed to have direct effects on neurons. IL-1β could increase the neuronal vulnerability to the Aβ toxicity. IL-6 has been shown to selectively enhance the calcium response of neurons to the excitotoxic stimuli (Qiu et al., 1995). In the AD patients and murine models, plaque-associated microglia exhibit quite different phenotypes and activating status in the brain parenchyma, and there is evidence for the expression of both M1 and M2 (Colton et al., 2006). Large amount of evidence suggests that the endocannabinoid system potentially modulates the inflammatory responses predominantly by CB_2R, which is mainly expressed by the microglial cells in the central nervous system. However, the experimental data remain elusive concerning the microglial morphological properties in AD pathology, after the CB_2R deletion. Our results confirmed the activation of cortical microglia after the CB_2R deletion. In addition, our results firstly identified the morphological changes of microglia in the prefrontal cortex. Meantime, the increased expression of pro-inflammatory cell surface markers were also observed in the prefrontal cortex after the CB_2R deletion, in both the Aβ-injected $CB_2R^{-/-}$ mice and CB_2R-deficient APP/PS1 mice, accompanied with the increased density of microglia and obvious morphological changes. We also found CB2R deletion did not affect inflammatory responses in the hippocampus of $A\beta_{1-42}$-injected AD mice in this study (Suppl. Fig. 3). Our results provided strong evidence that the CB_2R deletion led to regional selective activation of microglia due to the neurotoxicity induced by Aβ oligomers or plaques. Although direct evidence indicates that microglia have dynamitic processes and could constantly contact with neuronal synapses *in vivo*, whether and how microglia regulate the synaptic structure and function remain unclear(Colton et al., 2006; Wake et al., 2009). In this study, our results indicated that the CB_2R deletion increased the susceptibility of microglia morphological change in response to Aβ oligomers and plaques in the prefrontal cortex at the early stages of AD (Figs. 2 and 5). Our results provided strong evidence that the CB_2R deletion caused a regional selective microglial activation. In this study, we found CB_2R deletion did not influence Aβ plaque load in the prefrontal cortex in the APP/PS1mice (Suppl. Fig. 4 and Fig.5), but APP/PS1*CB2-/- mice showed a higher content of soluble $A\beta_{40}$ compared to APP/PS1 mice in the prefrontal cortex but not in the hippocampus (Suppl. Fig. 5). Furthermore, similar findings have been observed that the immune-related complement proteins or CX3CR1 receptor expressed on microglia have important impacts on the synapse dysfunction(Hoshiko et al., 2012; Schafer et al., 2012). Taken together, in addition to mediating the microglial dysfunction, whether and how the CB_2R pathway leads to the potential region-specific synaptic vulnerability in AD needs further investigation. There are conflicting

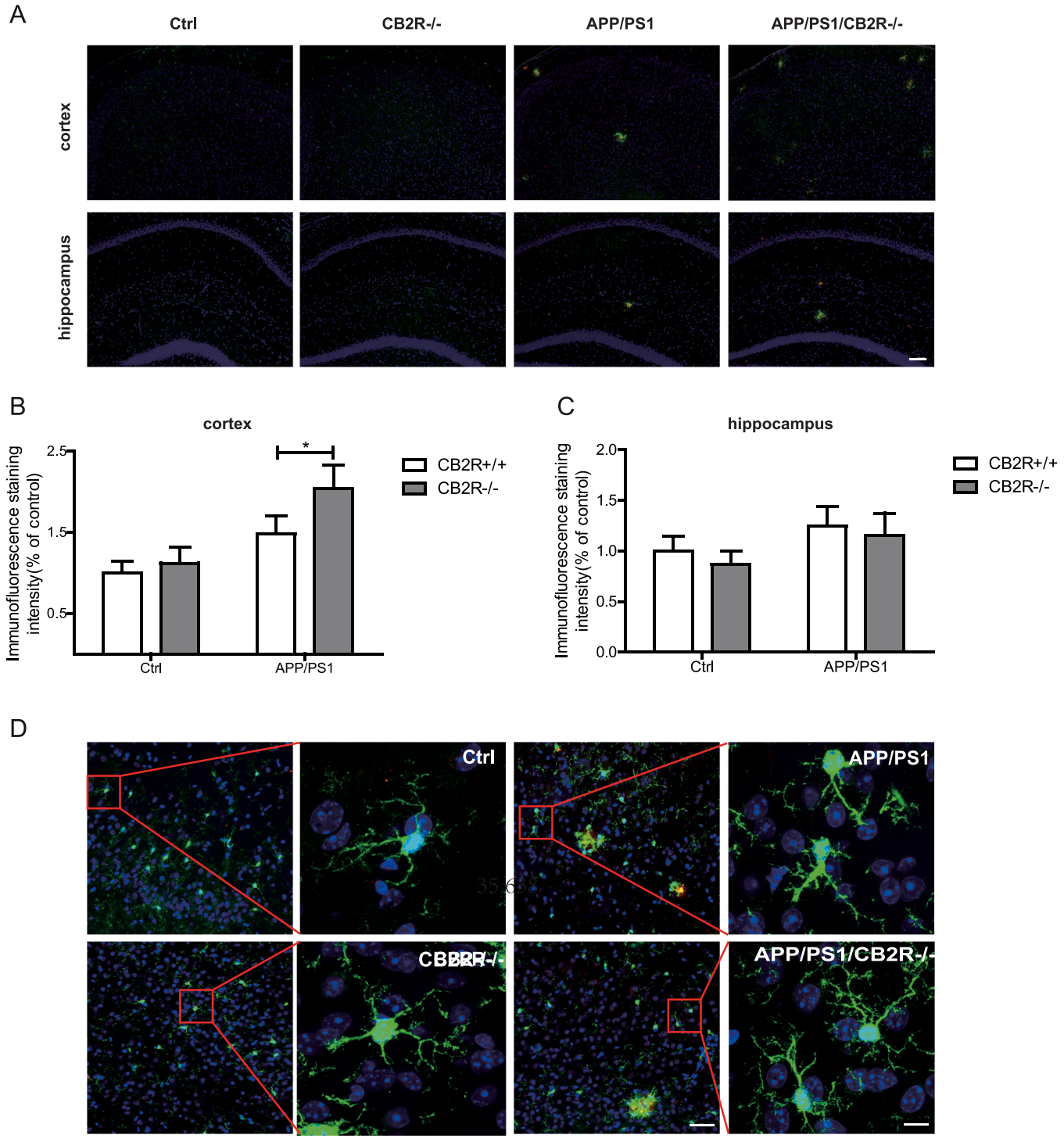

Fig. 5. Microglial immunoreactivity in APP/PS1 mice brain with or without CB2R deletion were measured by immunofluorescence staining. (A) Representative immunofluorescence images of microglia in the prefrontal cortex and hippocampus of control mice and APP/PS1 mice with or without CB2R deletion. Activated microglia were visualized with antibody Iba-1 in green, amyloid plaques were stained with the mouse monoclonal antibody 6E10 in red and nuclei were stained with DAPI in blue. Scale bar represents 100μm (original magnification 10×). Quantification of Iba-1 immunofluorescence intensity of all groups in the cortex (B) and hippocampus(C), presented as percentage of control mice. (D) Microglia morphological features were observed under confocal laser scanning microscopy. Panels to the right show high-magnification images of the cortical areas indicated by frames in the left panels. Scale bar represents 50μm (original magnification 20×) in left row, and Scale bar represents 10μm (original magnification 100×) in right row.*$P<0.05$, compared with APP/PS1 mice. Data were analyzed by Two-way ANOVA. Results are expressed as mean±SEM (n=4–6).

results regarding the effects of CB_2R deletion in CB_2R-deficient APP/PS1 mouse models. It has been reported that the CB_2R deletion in the APP/PS1 transgenic mouse model of AD reduces the microglial response to the Aβ deposition, rather than the astrocytes(Aso et al., 2016; Schmole et al., 2015). In this study, it was remarkable that the microglia in the prefrontal cortex exhibited differential activation to the cytokines in the absence of CB_2R. CB_2R participates in the regulation of neuro-inflammation, which regulates the susceptibility to Aβ toxicity, thus

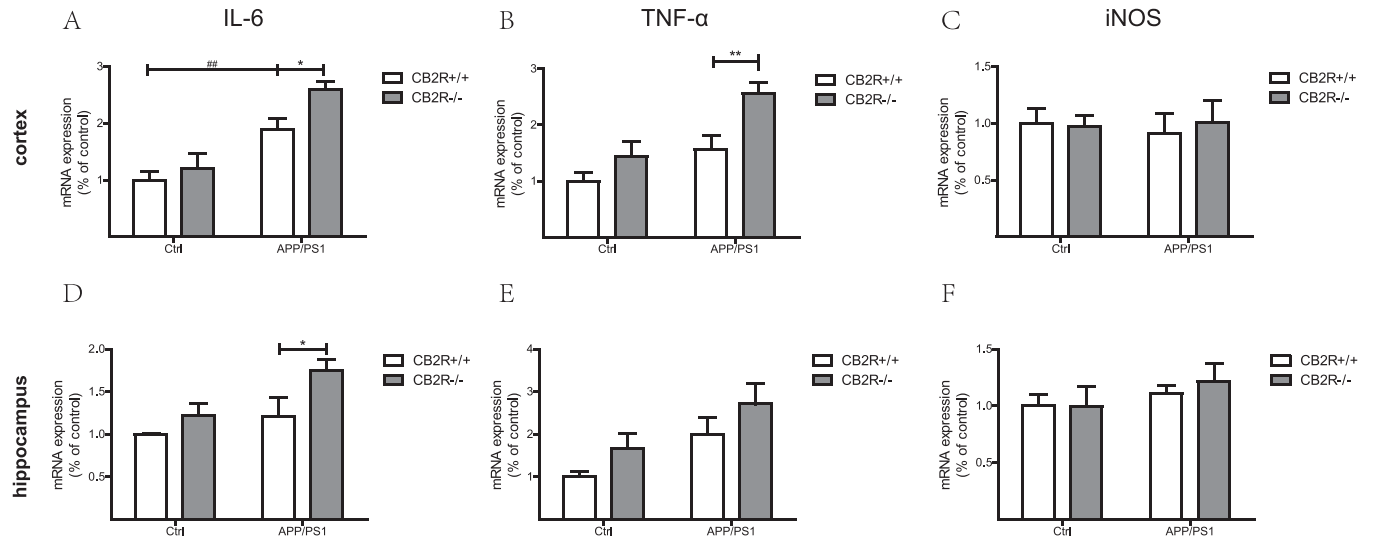

Fig. 6. Proinflammatory mediators mRNA expression level assessed by quantitative real-time PCR in APP/PS1 mice brain with or without CB2R deletion. Quantification of IL-6(A、D), TNF-α(B、E) and iNOS (C、F) mRNA levels in the prefrontal cortex and hippocampus of control mice and APP/PS1 mice with or without CB2R deletion. The mRNA expression levels of interest genes were normalized against GAPDH and presented percentage of Control mice. $^{\#\#}P<0.01$, compared with C57BL/J control mice ; $^{*}P<0.05$, $^{**}P<0.01$compared with APP/PS1 mice., Data were analyzed by Two-way ANOVA. Results are expressed as mean±SEM (n=4–6).

accelerating the disease progression. Although astrocytes were abundant and play multiple roles in the brain, our data demonstrated that the GFAP immunoreactivity was not affected in the $CB_2R^{-/-}$ mice injected with Aβ (Suppl. Fig. 1). Although the GFAP immunoreactivity in both Aβ-injected WT and APP/PS1 mice was significantly increased, our data demonstrated that the CB_2R deletion did not induce any significant changes in the astrocyte density in the prefrontal cortex or hippocampus, in the Aβ-injected $CB_2R^{-/-}$ and APP/PS1*$CB_2R^{-/-}$mice. Therefore, active astrocytes did not aggravate the dysfunctional inflammation status, and thus appearing to play a smaller role in AD when CB_2R was deleted. Actually, similar findings were also observed in the mouse models of acute sepsis. The CB_2R knockout mice were vulnerable for lipopolysaccharide (LPS)-induced inflammation (Gui et al., 2013). Region-specifically increased neutrophil recruitment and pro-inflammatory chemokine expression have been observed in the spleen of CB_2R knockout mice, during the acute systemic inflammation induced by the LPS insult (Kapellos et al., 2017; Turcotte et al., 2016). In the Huntington's disease, similar findings have been reported that the genetic ablation of CB_2R enhances the microglial activation and exacerbates the disease symptoms(Palazuelos et al., 2009).

Taken together, our results indicated that the CB_2R deletion played an important role in the acute phase or at the early stage of AD pathology, mainly targeting on the microglial function under Aβ neurotoxicity. The region-specific vulnerability of the endocannabinoid system in AD might be due to the higher baseline rates of metabolic and neural activity in the prefrontal cortex in response to Aβ neurotoxicity, compared with the hippocampus. Future studies are still needed to explore the factors contributing to the vulnerability of inflammation in the case of CB_2R deletion.

CRediT authorship contribution statement

Tong Zhang: Data curation. **JiaGuang Sun:** Data curation, Formal analysis, Investigation, Methodology. **Qiang Jiao:** Validation. **Shuai-Chen Li:** Writing - review & editing. **XiangBo Meng:** Writing - review & editing. **JingPu Shi:** Conceptualization, Data curation. **Bo Wang:** Writing – original draft.

Declaration of Competing Interest

The authors declare that they have no known competing financial interests or personal relationships that could have appeared to influence the work reported in this paper

Acknowledgments

This work was supported by a grant from the Natural Science Foundation of China (81471233) and Beijing Municipal Science and Technology Commission project (Z121102002512046).

Appendix A. Supporting information

Supplementary data associated with this article can be found in the online version at doi:10.1016/j.ibneur.2024.08.004.

References

Aso, E., Andres-Benito, P., Carmona, M., Maldonado, R., Ferrer, I., 2016. Cannabinoid receptor 2 participates in amyloid-beta processing in a mouse model of Alzheimer's disease but plays a minor role in the therapeutic properties of a cannabis-based medicine. J. Alzheimers Dis. *51* (2), 489–500. https://doi.org/10.3233/JAD-150913.

Aso, E., Juves, S., Maldonado, R., Ferrer, I., 2013. CB2 cannabinoid receptor agonist ameliorates Alzheimer-like phenotype in AbetaPP/PS1 mice. J. Alzheimers Dis. *35* (4), 847–858. https://doi.org/10.3233/JAD-130137.

Benito, C., Nunez, E., Tolon, R.M., Carrier, E.J., Rabano, A., Hillard, C.J., Romero, J., 2003. Cannabinoid CB2 receptors and fatty acid amide hydrolase are selectively overexpressed in neuritic plaque-associated glia in Alzheimer's disease brains. J. Neurosci. *23* (35), 11136–11141. https://doi.org/10.1523/JNEUROSCI.23-35-11136.2003.

Bolmont, T., Haiss, F., Eicke, D., Radde, R., Mathis, C.A., Klunk, W.E., Kohsaka, S., Jucker, M., Calhoun, M.E., 2008. Dynamics of the microglial/amyloid interaction indicate a role in plaque maintenance. J. Neurosci. *28* (16), 4283–4292. https://doi.org/10.1523/JNEUROSCI.4814-07.2008.

Citron, M., 2010. Alzheimer's disease: strategies for disease modification. Nat. Rev. Drug Discov. *9* (5), 387–398. https://doi.org/10.1038/nrd2896.

Colton, C.A., Mott, R.T., Sharpe, H., Xu, Q., Van Nostrand, W.E., Vitek, M.P., 2006. Expression profiles for macrophage alternative activation genes in AD and in mouse models of AD. J. Neuroinflamm. *3*, 27. https://doi.org/10.1186/1742-2094-3-27.

Crews, L., Masliah, E., 2010. Molecular mechanisms of neurodegeneration in Alzheimer's disease. Hum. Mol. Genet *19* (R1), R12–R20. https://doi.org/10.1093/hmg/ddq160.

Frank-Cannon, T.C., Alto, L.T., McAlpine, F.E., Tansey, M.G., 2009. Does neuroinflammation fan the flame in neurodegenerative diseases? Mol. Neurodegener. *4*, 47. https://doi.org/10.1186/1750-1326-4-47.

Gui, H., Sun, Y., Luo, Z.M., Su, D.F., Dai, S.M., Liu, X., 2013. Cannabinoid receptor 2 protects against acute experimental sepsis in mice. Mediat. Inflamm. *2013* (1), 741303, 2013,(2013-5-28).

Harry, G.J., Kraft, A.D., 2012. Microglia in the developing brain: a potential target with lifetime effects. Neurotoxicology *33* (2), 191–206. https://doi.org/10.1016/j.neuro.2012.01.012.

Hoshiko, M., Arnoux, I., Avignone, E., Yamamoto, N., Audinat, E., 2012. Deficiency of the microglial receptor CX3CR1 impairs postnatal functional development of thalamocortical synapses in the barrel cortex. J. Neurosci. *32* (43), 15106–15111. https://doi.org/10.1523/JNEUROSCI.1167-12.2012.

Irit, A., Mouna, M., 2006. Ventromedial prefrontal cortex is obligatory for consolidation and reconsolidation of object recognition memory. Cereb. Cortex *16* (12), 1759–1765.

Kapellos, T.S., Recio, C., Greaves, D.R., Iqbal, A.J., 2017. Cannabinoid Receptor 2 Modulates Neutrophil Recruitment in a Murine Model of Endotoxemia. Mediat. Inflamm. *2017* (5), 1–15.

Kwon, H.S., Koh, S.H., 2020. Neuroinflammation in neurodegenerative disorders: the roles of microglia and astrocytes. Transl. Neurodegener. *9* (1), 42. https://doi.org/10.1186/s40035-020-00221-2.

Li, C., Shi, J., Wang, B., Li, J., Jia, H., 2019. CB2 cannabinoid receptor agonist ameliorates novel object recognition but not spatial memory in transgenic APP/PS1 mice. Neurosci. Lett. *707*, 134286 https://doi.org/10.1016/j.neulet.2019.134286.

Martin-Moreno, A.M., Brera, B., Spuch, C., Carro, E., Garcia-Garcia, L., Delgado, M., Pozo, M.A., Innamorato, N.G., Cuadrado, A., de Ceballos, M.L., 2012. Prolonged oral cannabinoid administration prevents neuroinflammation, lowers beta-amyloid levels and improves cognitive performance in Tg APP 2576 mice. J. Neuroinflamm. *9*, 8. https://doi.org/10.1186/1742-2094-9-8.

Meyer-Luehmann, M., Spires-Jones, T.L., Prada, C., Garcia-Alloza, M., de Calignon, A., Rozkalne, A., Koenigsknecht-Talboo, J., Holtzman, D.M., Bacskai, B.J., Hyman, B.T., 2008. Rapid appearance and local toxicity of amyloid-beta plaques in a mouse model of Alzheimer's disease. Nature *451* (7179), 720–724. https://doi.org/10.1038/nature06616.

Miller, A.M., Stella, N., 2008. CB2 receptor-mediated migration of immune cells: it can go either way. Br. J. Pharm. *153* (2), 299–308. https://doi.org/10.1038/sj.bjp.0707523.

Morcuende, A., Garcia-Gutierrez, M.S., Tambaro, S., Nieto, E., Manzanares, J., Femenia, T., 2022. Immunomodulatory role of CB2 receptors in emotional and cognitive disorders. Front. Psychiatry *13*, 866052. https://doi.org/10.3389/fpsyt.2022.866052.

Morris, R.G., Inglis, J., Ainge, J.A., Olverman, H.J., Tulloch, J., Dudai, Y., Kelly, P.A., 2006. Memory reconsolidation: sensitivity of spatial memory to inhibition of protein synthesis in dorsal hippocampus during encoding and retrieval. Neuron *50* (3), 479–489. https://doi.org/10.1016/j.neuron.2006.04.012.

Nakajima, K., Kohsaka, S., 2001. Microglia: activation and their significance in the central nervous system. J. Biochem. *130* (2), 169–175.

Palazuelos, J., Aguado, T., Pazos, M.R., Julien, B., Carrasco, C., Resel, E., Sagredo, O., Benito, C., Romero, J., Azcoitia, I., Fernandez-Ruiz, J., Guzman, M., Galve-Roperh, I., 2009. Microglial CB2 cannabinoid receptors are neuroprotective in Huntington's disease excitotoxicity. Brain *132* (Pt 11), 3152–3164. https://doi.org/10.1093/brain/awp239.

Qiu, Z., Parsons, K.L., Gruol, D.L., 1995. Interleukin-6 selectively enhances the intracellular calcium response to NMDA in developing CNS neurons. J. Neurosci. Off. J. Soc. Neurosci. *15* (10), 6688.

Rossato, J.I., Bevilaqua, L.R., Medina, J.H., Izquierdo, I., Cammarota, M., 2006. Retrieval induces hippocampal-dependent reconsolidation of spatial memory. Learn Mem. *13* (4), 431–440. https://doi.org/10.1101/lm.315206.

Schafer, D.P., Lehrman, E.K., Kautzman, A.G., Koyama, R., Mardinly, A.R., Yamasaki, R., Ransohoff, R.M., Greenberg, M.E., Barres, B.A., Stevens, B., 2012. Microglia sculpt postnatal neural circuits in an activity and complement-dependent manner. Neuron *74* (4), 691–705. https://doi.org/10.1016/j.neuron.2012.03.026.

Schmole, A.C., Lundt, R., Ternes, S., Albayram, O., Ulas, T., Schultze, J.L., Bano, D., Nicotera, P., Alferink, J., Zimmer, A., 2015. Cannabinoid receptor 2 deficiency results in reduced neuroinflammation in an Alzheimer's disease mouse model. Neurobiol. Aging *36* (2), 710–719. https://doi.org/10.1016/j.neurobiolaging.2014.09.019.

Selkoe, D.J., 2001. Alzheimer's disease: genes, proteins, and therapy. Physiol. Rev. *81* (2), 741–766. https://doi.org/10.1152/physrev.2001.81.2.741.

Solas, M., Francis, P.T., Franco, R., Ramirez, M.J., 2013. CB2 receptor and amyloid pathology in frontal cortex of Alzheimer's disease patients. Neurobiol. Aging *34* (3), 805–808. https://doi.org/10.1016/j.neurobiolaging.2012.06.005.

Stempel, A.V., Stumpf, A., Zhang, H.Y., Ozdogan, T., Pannasch, U., Theis, A.K., Otte, D. M., Wojtalla, A., Racz, I., Ponomarenko, A., Xi, Z.X., Zimmer, A., Schmitz, D., 2016. Cannabinoid Type 2 Receptors Mediate a Cell Type-Specific Plasticity in the Hippocampus. Neuron *90* (4), 795–809. https://doi.org/10.1016/j.neuron.2016.03.034.

Tolon, R.M., Nunez, E., Pazos, M.R., Benito, C., Castillo, A.I., Martinez-Orgado, J.A., Romero, J., 2009. The activation of cannabinoid CB2 receptors stimulates in situ and in vitro beta-amyloid removal by human macrophages. Brain Res. *1283*, 148–154. https://doi.org/10.1016/j.brainres.2009.05.098.

Tomiyama, T., Matsuyama, S., Iso, H., Umeda, T., Takuma, H., Ohnishi, K., Ishibashi, K., Teraoka, R., Sakama, N., Yamashita, T., Nishitsuji, K., Ito, K., Shimada, H., Lambert, M.P., Klein, W.L., Mori, H., 2010. A mouse model of amyloid beta oligomers: their contribution to synaptic alteration, abnormal tau phosphorylation, glial activation, and neuronal loss in vivo. J. Neurosci. *30* (14), 4845–4856. https://doi.org/10.1523/JNEUROSCI.5825-09.2010.

Turcotte, C., Blanchet, M.R., Laviolette, M., Flamand, N., 2016. The CB 2 receptor and its role as a regulator of inflammation. Cell. Mol. Life Sci. *73* (23), 4449–4470.

Wake, H., Moorhouse, A.J., Jinno, S., Kohsaka, S., Nabekura, J., 2009. Resting microglia directly monitor the functional state of synapses in vivo and determine the fate of ischemic terminals. J. Neurosci. *29* (13), 3974–3980. https://doi.org/10.1523/JNEUROSCI.4363-08.2009.

Zhang, F., Vadakkan, K.I., Kim, S.S., Wu, L.J., Shang, Y., Zhuo, M., 2008. Selective activation of microglia in spinal cord but not higher cortical regions following nerve injury in adult mouse. Mol. Pain. *4*, 15. https://doi.org/10.1186/1744-8069-4-15.